Assessment of Rod, Cone, and Intrinsically Photosensitive Retinal Ganglion Cell Contributions to the Canine Chromatic Pupillary Response

Connie Y. Yeh,[1,2] Kristin L. Koehl,[1] Christine D. Harman,[1] Simone Iwabe,[2] José M. Guzman,[2] Simon M. Petersen-Jones,[1] Randy H. Kardon,[3,4] and András M. Komáromy[1,2]

[1]College of Veterinary Medicine, Michigan State University, East Lansing, Michigan, United States
[2]School of Veterinary Medicine, University of Pennsylvania, Philadelphia, Pennsylvania, United States
[3]Department of Ophthalmology and Visual Sciences, University of Iowa, Iowa City, Iowa, United States
[4]Veterans Affairs Health Care System, Iowa City, Iowa, United States

Correspondence: András M. Komáromy, Veterinary Medical Center, 736 Wilson Road, Room D-208, East Lansing, MI 48824, USA; komaromy@cvm.msu.edu.

Submitted: May 4, 2016
Accepted: November 17, 2016

Citation: Yeh CY, Koehl KL, Harman CD, et al. Assessment of rod, cone, and intrinsically photosensitive retinal ganglion cell contributions to the canine chromatic pupillary response. *Invest Ophthalmol Vis Sci*. 2017;58:65–78. DOI:10.1167/iovs.16-19865

Purpose. The purpose of this study was to evaluate a chromatic pupillometry protocol for specific functional assessment of rods, cones, and intrinsically photosensitive retinal ganglion cells (ipRGCs) in dogs.

Methods. Chromatic pupillometry was tested and compared in 37 dogs in different stages of primary loss of rod, cone, and combined rod/cone and optic nerve function, and in 5 wild-type (WT) dogs. Eyes were stimulated with 1-s flashes of dim (1 cd/m^2) and bright (400 cd/m^2) blue light (for scotopic conditions) or bright red (400 cd/m^2) light with 25-cd/m^2 blue background (for photopic conditions). Canine retinal melanopsin/*Opn4* was cloned, and its expression was evaluated using real-time quantitative reverse transcription-PCR and immunohistochemistry.

Results. Mean ± SD percentage of pupil constriction amplitudes induced by scotopic dim blue (scDB), scotopic bright blue (scBB), and photopic bright red (phBR) lights in WT dogs were 21.3% ± 10.6%, 50.0% ± 17.5%, and 19.4% ± 7.4%, respectively. Melanopsin-mediated responses to scBB persisted for several minutes (7.7 ± 4.6 min) after stimulus offset. In dogs with inherited retinal degeneration, loss of rod function resulted in absent scDB responses, followed by decreased phBR responses with disease progression and loss of cone function. Primary loss of cone function abolished phBR responses but preserved those responses to blue light (scDB and scBB). Although melanopsin/*Opn4* expression was diminished with retinal degeneration, melanopsin-expressing ipRGCs were identified for the first time in both WT and degenerated canine retinas.

Conclusions. Pupil responses elicited by light stimuli of different colors and intensities allowed differential functional assessment of canine rods, cones, and ipRGCs. Chromatic pupillometry offers an effective tool for diagnosing retinal and optic nerve diseases.

Keywords: canine, chromatic pupillometry, intrinsically photosensitive retinal ganglion cells, melanopsin, retinal dystrophy

The pupillary light reflex (PLR) informs about retinal and visual pathway functions, and it is routinely evaluated during clinical ophthalmic examination. Pupillometry enables precise quantification of changes in pupil size for clinical and research purposes, improving upon traditional qualitative PLR testing based on gross observations of pupillary responses. The discovery of a subset of retinal ganglion cells (RGCs) known as intrinsically photosensitive RGCs (ipRGCs) provided new understanding of the PLR.[1] The ipRGC's unique photopigment melanopsin, with a peak spectral sensitivity of ~480 nm, may provide a basis for using blue light PLR to differentiate diseases affecting inner retina, optic nerve, and central nervous system.[2–7] Subsequently, chromatic pupillometry using red and blue light stimuli was developed in humans to permit detailed testing of retinal cell subpopulations: pupil constriction evaluated in the dark by dim and bright blue light stimuli (scotopic dim blue [scDB] and scotopic bright blue [scBB]) specifically measures rod- and ipRGC-mediated functions, respectively, whereas a bright red light stimulus with a blue-lit background (photopic bright red [phBR]) specifically measures cone function.[8–10]

Chromatic pupillometry has also been introduced for assessment of the visual pathway in the dog,[11–13] an important model species for inherited blinding disorders[14,15]; however, the respective contributions of different canine cell populations to specific colored light responses are unknown. In this study, we assessed the validity of a human chromatic pupillometry[10] protocol in dogs in order to test the hypothesis that the differential contributions of rods, cones, and ipRGCs to canine pupillary responses could be specifically analyzed using blue and red light stimuli. To test our approach and hypothesis, we took advantage of the unique availability of an unparalleled group of well-characterized canine retinal and optic nerve disease models at Michigan State University and University of

Table. Summary of Study Dogs

Disease	Mutated Gene	Functional Change	Dog	Sex	Age, y
WT			N1	F	1
			N2	F	1
			N3	F	0.6
			N4	M	1
			N5‖	F	2.5
			N6*	F	0.8
			N7*	M	0.8
CNGB1-PRA	*CNGB1*	↓ Rod function	1CNGB1	M	0.3
			2CNGB1	M	5.2
CNGB3-ACHM	*CNGB3*	↓ Cone function	1CNGB3*	M	4.8
			2CNGB3	F	4.6
			3CNGB3‖	M	1.6
			4CNGB3	F	1.3
			5CNGB3‖	M	1.4
			6CNGB3*	M	0.6
PDE6B-rcd1 (young)	*PDE6B*	↓ Rod function	1PDE6B†	M	0.7
			2PDE6B	F	0.7
			3PDE6B†	F	0.4
PDE6B-rcd1 (old)	*PDE6B*	↓ Rod and cone function	4PDE6B†	F	6
			5PDE6B	F	5.3
RD3-rcd2 (old)	*RD3*	↓ Rod and cone function	1RD3	M	1.3
			3RD3†	F	3.7
			4RD3	F	3.4
PDE6A-rcd3 (young)	*PDE6A*	↓ Rod function	1PDE6A†	F	0.7
PDE6A-rcd3 (old)	*PDE6A*	↓ Rod and cone function	2PDE6A	M	3.8
RPE65-LCA	*RPE65*	↓ Rod and cone function	1RPE65†	F	4.4
			2RPE65†	F	4.4
			3RPE65†	F	2.1
			4RPE65†	F	0.8
			5RPE65†	F	0.8
			6RPE65†	F	0.8
PRCD-prcd	*PRCD*	↓ Rod and cone function	1PRCD†‡	F	8.3
			2PRCD	M	5.9
IQCB1-crd2	*IQCB1*	↓ Rod and cone function	1crd2†	F	1.5
			2crd2	F	1.5
			3crd2†	M	3.8
			4crd2	M	3.8
STK38L-erd	*STK38L*	↓ Rod and cone function	1erd‡	M	8.4
			2erd†	M	3.5
			3erd	M	3.5
RPGR-XLPRA2	*RPGR*	↓ Rod and cone function	1XLPRA2†	F	7.2
			2XLPRA2	F	6.5
			3XLPRA2	F	5.8
RD3-rcd2 (old) and *NEHJ1*-CEA	*RD3* and *NEHJ1*	↓ Rod, cone, and RGC function	2RD3§	M	3.3

* Light intensity series was performed with multiple increases in stimulus intensity.
† ERG was completed during the same session as pupillometry.
‡ IHC was available.
§ Animal also had severe optic nerve head coloboma.
‖ Chromatic pupillometry reproducibility evaluated by repeat testing within 4 to 5 months.

Pennsylvania. Furthermore, in order to complement our functional results, we cloned the canine melanopsin/*Opn4* gene and demonstrated for the first time melanopsin-expressing ipRGC in the normal and the diseased canine retina.

Methods

Animals

We compared results of chromatic pupillometry testing in 37 dogs with different stages of primary loss of rod, cone, combined rod/cone, and optic nerve functions with those in 5 wild-type (WT) dogs (Table). Diseases included *CNGB1*-progressive retinal atrophy (PRA), *CNGB3* achromatopsia (ACHM), *PDE6B* rod/cone dysplasia 1 (rcd1), *RD3* rod/cone dysplasia 2 (rcd2), *PDE6A* rod/cone dysplasia 3 (rcd3), *RPE65* Leber congenital amaurosis (LCA), *PRCD* progressive rod/cone degeneration (prcd), *IQCB1* cone/rod dystrophy 2 (crd2), *RPGR*-X-linked progressive retinal atrophy 2 (XLPRA2), *STK38L* early retinal degeneration (erd), and *NEHJ1* Collie eye anomaly (CEA).[16–39] Dogs were grouped and tested based on 4 previously reported retinal and optic nerve disease phenotypes, as follows: (1) Group 1 consisted of primary loss of rod function in dogs with *CNGB1*-PRA and young (<1 year of age) dogs with *PDE6A*-rcd3 and *PDE6B*-rcd1; (2) group 2 included primary loss of cone function in dogs with *CNGB3*-

ACHM; (3) group 3 contained various severities of combined loss of rod and cone function in older dogs affected with *PDE6B*-rcd1, *RD3*-rcd2, and *PDE6A*-rcd3, and dogs affected with *RPE65*-LCA, *PRCD*-prcd, *IQCB1*-crd2, *STK38L*-erd, and *RPGR*-XLPRA2; (4) and group 4 included primary loss of optic nerve function in 1 dog with severe optic nerve head coloboma due to *NEHJ1*-CEA, which was also affected by *RD3*-rcd2. We also assessed pupillary responses to differential blue and red light intensities in 2 additional WT and 2 *CNGB3*-mutant dogs.

We performed complete ophthalmic examinations, including vision assessment by testing the menace response, slit lamp biomicroscopy (model SL15; Kowa Optimed, Inc., Torrance, CA, USA), indirect ophthalmoscopy (All Pupil II; Keeler Instruments, Inc., Broomall, PA, USA), and retinal photography (RetCamII; Clarity Medical Systems, Pleasanton, CA, USA) on all dogs included in this part of the study.

For molecular studies, 23 additional dogs, including WT dogs and those with different stages of retinal diseases, were used (17 for sequencing/cloning and real-time quantitative reverse transcription-PCR [qRT-PCR] and 6 for immunohistochemistry [IHC]) (Supplementary Table S1). We performed chromatic pupillometry on two of the dogs used for IHC. Dogs were enucleated immediately after euthanasia performed using an intravenous overdose of sodium pentobarbital (≥85 mg/kg; Fatal-Plus, Vortech, Pharmaceutical, Ltd., Dearborn, MI, USA). All studies were performed in compliance with ARVO Statement for the Use of Animals in Ophthalmic and Vision Research and were approved by Michigan State University and University of Pennsylvania Institutional Animal Care and Use Committees.

Anesthesia

In an initial pilot study, 5 dogs underwent chromatic pupillometry recordings using injectable chemical restraint alone with intravenously administered dexmedetomidine (4 μg/kg; Dexdomitor; Zoetis, Florham Park, NJ, USA). This sedation alone was insufficient for reliable PLR recordings due to persistent fluctuations in pupil size and eye movements. Therefore, for all pupillometry recording sessions, dogs received isoflurane gas anesthesia and were positioned in sternal recumbency on a custom-made table equipped with a head rest. They were first premedicated using acepromazine, at an intravenous dose of 0.02 mg/kg (AceproJect; Henry Schein, Dublin, OH, USA) and induced with propofol (Propoflo 28; Abbott, Abbott Park, IL, USA) given intravenously to effect (starting dose, 4 mg/kg). The dogs were then intubated, and general anesthesia was maintained with isoflurane (2%–3% vaporizer setting; Isothesia; Henry Schein) in oxygen. Heart rate, respiratory rate, and body temperature were monitored throughout the procedure. A portable multiparameter veterinary monitor (model PM-9000Vet; Shenzhen Mindray; Bio-Medical Electronics, Co., Ltd., Nanshan, Shenzhen, PR, China) was used to assess blood pressure, oxygen saturation, and end-tidal CO_2. Anesthesia level was evaluated by monitoring changes in respiration or heart rate.

Chromatic Pupillometry

Both the left and right eyes were tested in each dog. The right eye was tested first. A Barraquer eyelid speculum was inserted to prevent interference by nictitating membrane and eyelids. Stay sutures (4-0 Perma-Hand Silk; Ethicon, Inc., Somerville, NJ, USA) were placed in the superior and inferonasal bulbar conjunctiva 2 mm posterior to the limbus. The stay sutures allowed globe manipulation and maintenance of the pupil in the central optical axis for pupillometry recording. The eye was lubricated (Optixcare Eye Lube; CLC Medica, Waterdown, Ontario, Canada) prior to the start of recording. The untested eye was covered with a black plastic ocular shield (Oculo-Plastik, Inc., Montréal, Canada) which contained a hypermellose 2.5% ophthalmic demulcent (Goniosoft; OCuSOFT, Inc., Rosenberg, TX, USA). After the right eye was tested, the left eye was tested using the same procedure.

Recordings were performed with the RETIport system using a Ganzfeld dome (Roland Consult, Havel, Germany). This system allowed timed delivery of a light-emitting diode (LED) light of a particular wavelength and intensity. An infrared-sensitive camera located within the Ganzfeld dome was used for real-time pupil recording. The system contained an automatic pupil detector that measured pupil size throughout recording, at a sample rate of 30 fps. The RETIport pupillometry system was developed for testing human subjects, but we found that actual canine pupil size correlated linearly with the system's measurements, the machine consistently overestimating pupil size by ~33% (Supplementary Fig. S1). Actual pupil size was measured using a ruler placed temporal to the eye when the dog's head was in the Ganzfeld dome. Because this pupillometry system was new, we continued to improve its adaptation for use in animals in collaboration with the manufacturer (Roland Consult).

Testing parameters were adapted from a previously published human protocol.[10] After 10 min of dark adaptation (scotopic conditions), the eye was stimulated first with a 1-s flash of dim blue light (scDB: 1 cd/m^2, 470 nm) and then a 1-s flash of bright blue light (scBB: 400 cd/m^2, 470nm) following pupil recovery to baseline. After 5 min of light adaptation to a blue background (480 nm, 25 cd/m^2) the eye was stimulated with a 1-s flash of bright red light (phBR: 400 cd/m^2, 640 nm). The blue background light remained on throughout photopic-condition testing. Duplicate tests were performed for each light intensity tested in each eye, and the results were averaged. These intensities were photopically matched for the human eye, and we also found good agreement with canine spectral sensitivity (see Fig. 6).

During our evaluation of the system, we noted that, in dogs that retained cone function, a small light artifact (movement of the pupil detector) was observed for several milliseconds after onset of the bright red light stimulus but that the pupil response quickly overcame the artifact. In dogs with no cone function, the light artifact was seen throughout the time the bright red light stimulus was on. Due to the light artifact, we found that it was important to observe the real-time video recording of the bright red light testing with blue background to differentiate between light artifact and true pupil response.

Test-retest variability was assessed in 3 dogs (Table) by repeating the chromatic pupillometry testing protocol 4 to 5 months after the first recording (see Supplementary Fig. S5).

To determine if variations in constriction amplitude found between the WT dogs could be due to entrance pupil size, pupil responses were measured over a range of light intensity stimuli, under both scotopic and photopic conditions for the right eyes of 2 WT dogs and 2 *CNGB3* mutant dogs. After 10 min of dark adaptation, alternating red and blue light stimuli were presented over an intensity range of 1 to 400 cd/m^2 in ~0.5-log steps (Supplementary Table S2). Light stimulus duration of 1 s was used. Duplicate tests were performed at each light intensity. We followed the protocol described above for the photopic condition, except that we added a blue background light to suppress rod function: The eyes were allowed to adapt for 5 min to the blue background light (25 cd/m^2) prior to testing, and the background light remained on throughout this testing.

Investigative Ophthalmology & Visual Science

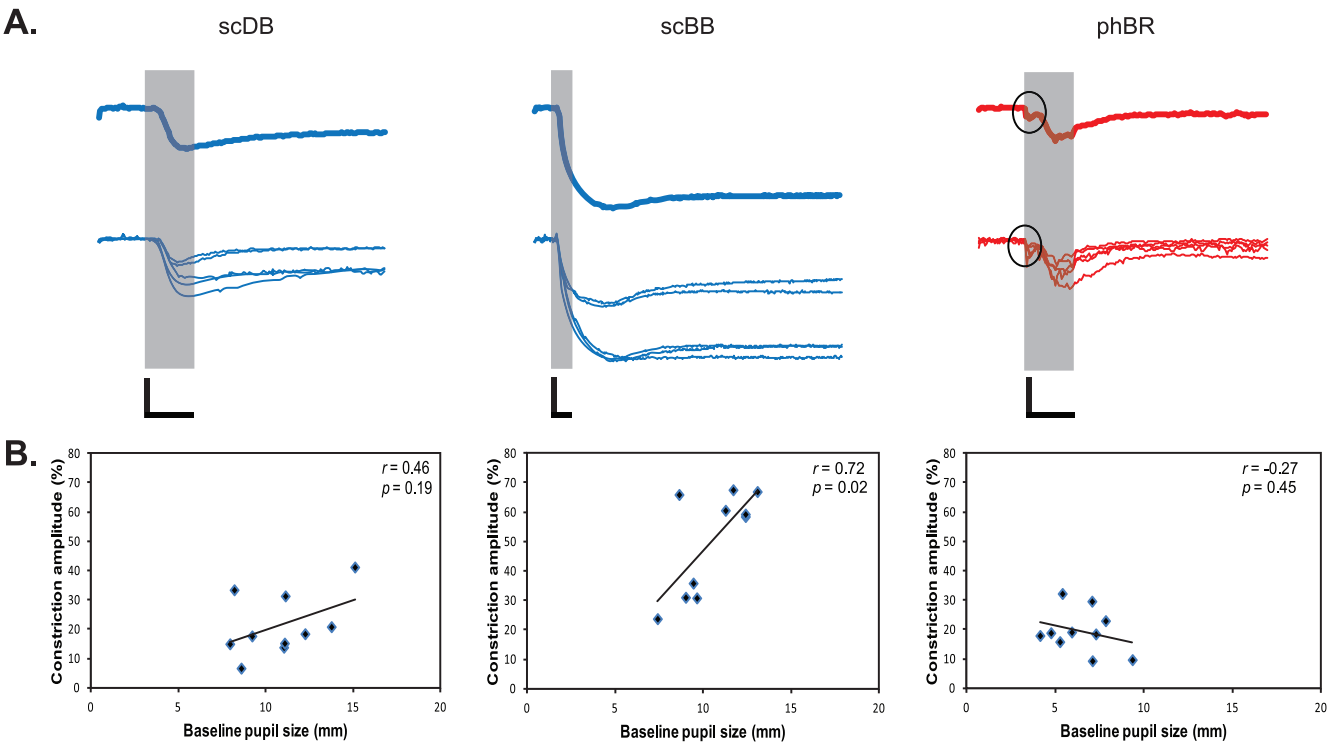

Figure 1. (**A**) Average (*top row*, *bold traces*) and individual (*bottom row*) PLRs in WT dogs. The *gray-shaded* area represent the 1-s light stimulus presentation. *Open circles* indicate the light artifact. (**B**) Correlation between baseline pupil size and constriction amplitude are shown with regression lines for WT dogs. *Calibration bars*: 1 s (time, *horizontal*) and 20% (normalized pupil size, *vertical*).

Data Analysis

Data were exported to Excel software (Microsoft, Redmond, WA, USA) for analysis. Absolute PLRs were recorded and averaged for the duplicate tests at each light intensity. Baseline pupil size was taken as the median pupil size during the 1-s interval preceding onset of each respective stimulus. Normalized pupil size was then calculated by dividing the averaged absolute pupil size by the baseline pupil size. When both the right and the left eyes were tested, the normalized pupil sizes for both eyes were averaged. Maximum constriction amplitude was defined as the minimum pupil size attained after stimulus onset. Latency was defined as the time between stimulus onset and beginning of pupil constriction.[10] To determine the onset of the PLR, we attempted to use a method based on filtering, followed by first and second derivatives of pupil movement but found it was unsuccessful due to the low sample rate of 30 fps.[40] Therefore, we determined latency by measuring time from stimulus onset to the beginning of pupil constriction from each respective pupil response graph.

Anesthesia records of the tested dogs were evaluated to determine whether PLRs were affected by anesthesia level, by assessing heart rate, respiratory rate, isoflurane level, end tidal CO_2 level, and blood pressure.

Results are mean ± SD. Statistical significance of differences in latency and constriction amplitudes between WT dogs and affected dogs in the three different disease groups 1–3 for all testing protocols was determined by *F* test and unpaired Student's *t*-test or Mann-Whitney *U* test. The relationship between baseline pupil size and constriction amplitude was evaluated by Pearson correlation. Statistical computations were performed in Microsoft Excel, GraphPad (www.graphpad.com/quickcalcs/contMenu, in the public domain), and VassarStats (www.vassarstats.net/index.html, in the public domain). Differences were considered statistically significant for *P* values of <0.05.

Electroretinography

Standard scotopic and photopic full-field electroretinograms (ERG) were recorded in selected dogs (Table) under isoflurane anesthesia during the same chromatic pupillometry recording session, using the Ganzfeld dome system (Roland Consult), Jet contact lens electrodes (Fabrinal Eye Care, La Chaux-de-Fonds, Switzerland), and commercially available platinum subdermal needle electrodes (Grass Technologies, Warwick, RI, USA). In these dogs, chromatic pupillometry was only performed in one eye. The ERG was recorded first in the left eye followed by chromatic pupillometry in the right eye. The untested eye was covered with a black plastic ocular shield as described above. The left pupil was dilated with tropicamide 1% ophthalmic solution (Akorn Inc., Lake Forest, IL, USA) prior to electroretinography. Rod- and mixed cone/rod-mediated responses were recorded after 20 min of dark adaptation with scotopic single-white-flash stimuli at three different light luminances (0.01, 3, and 10 cds/m^2). Multiple responses (25 for the 0.01 cds/m^2 single-white-flash and 10 for the 3, and 10 cds/m^2 single white flash) were averaged. Following 10 min of light adaptation to white background illumination of 30 cd/m^2, cone-mediated signals were recorded in response to a 1-Hz single white flash (3 and 10 cds/m^2) and 30 Hz white flicker (3 cds/m^2). Multiple responses (10 for the 1-Hz single flash and 90 0.05-s sweeps for the 30-Hz flicker) were averaged.

Melanopsin/Opn4 Sequencing and Cloning

Normal retinas were collected from a WT dog and flash-frozen immediately following euthanasia. Total RNA was isolated from the retina by using TRIzol reagent (Invitrogen, Carlsbad, CA,

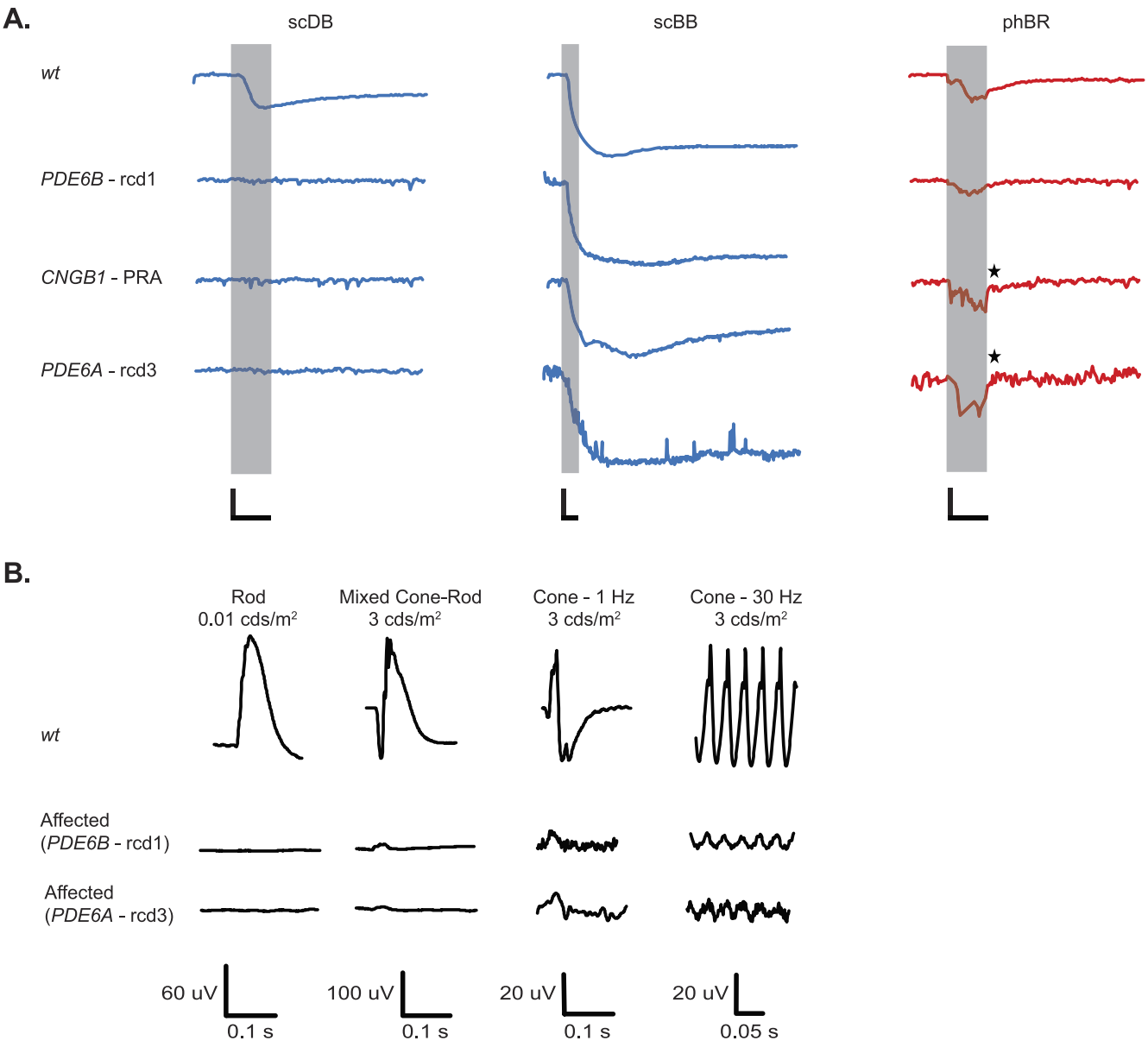

Figure 2. **(A)** Effects of mutations in *PDE6B*, *CNGB1*, and *PDE6A* on PLRs compared to average WT PLRs. Representative recordings are shown here. Recordings from all dogs are shown in Supplementary Figure S2. ★ indicates undetectable PLRs from *PDE6A*- and *CNGB1*-mutants overshadowed by a light artifact. *Shaded area* represents 1-s stimulus presentation. **(B)** Representative full-field ERGs. Compared to WT dogs, rod-mediated response were nonrecordable in young *PDE6B*- and *PDE6A*-mutants, whereas cone-mediated function was recordable but severely reduced in amplitude. **(A)** *Calibration bars*: 1 s (time, *horizontal*) and 20% (normalized pupil size, *vertical*).

USA) after homogenization. First-strand cDNA was synthesized from 2 μg of RNA, using High Capacity reverse transcription kit (Applied Biosystem, Waltham, MA, USA) according to the manufacturer's instructions. The resultant cDNA was used in a 50-μL PCR reaction assay, using FailSafe PCR system (Epicentra, Madison, WI, USA) with the custom-designed primers Mel_cDNAF (forward 5′-ACCACCCCCAGGATGAAC-3′) and Mel_cDNAR (reverse 5′-CTGCAGGCTTGTCCCTGT-3′). Primers were designed using Primer3 (http://frodo.wi.mit.edu, in the public domain) and the predicted canine sequence (CanFam 2.0) assembly (http://genome.ucsc.edu/cgi-bin/hgGateway, in the public domain). Each 50-μL reaction mixture contained PCR-grade water, FailSafe PCR enzyme mixture, 1 μL (100ng/μL) of DNA template, 1 μL of both forward and reverse primers, and one of the 12 different FailSafe PCR 2× PreMixes (A–L). PCR assay was performed under the following conditions: initial denaturation at 94°C for 3 min, then 94°C for 30 s, 58° for 1 min, and 72°C for 2 min for 35 cycles, followed by final extension at 72°C for 5 min.

Electrophoresis of PCR products was then carried out on a 1.5% agarose gel containing ethidium bromide, and a single DNA band of the correct size was observed for FailSafe PCR 2× PreMix G. The DNA was purified using the QIAquick gel Extraction Kit (QIAGEN, Inc., Germantown, MD, USA) according to the manufacturer's protocol. The purified 1,446-bp PCR product was cloned into the pCR4-TOPO TA vector using TOPO TA cloning kit (Thermo Fisher Scientific, Waltham, MA, USA) according to the provided protocol. The plasmid was prepared from an overnight culture, using the PureYield plasmid miniprep system (Promega, Madison, WI, USA), and 5

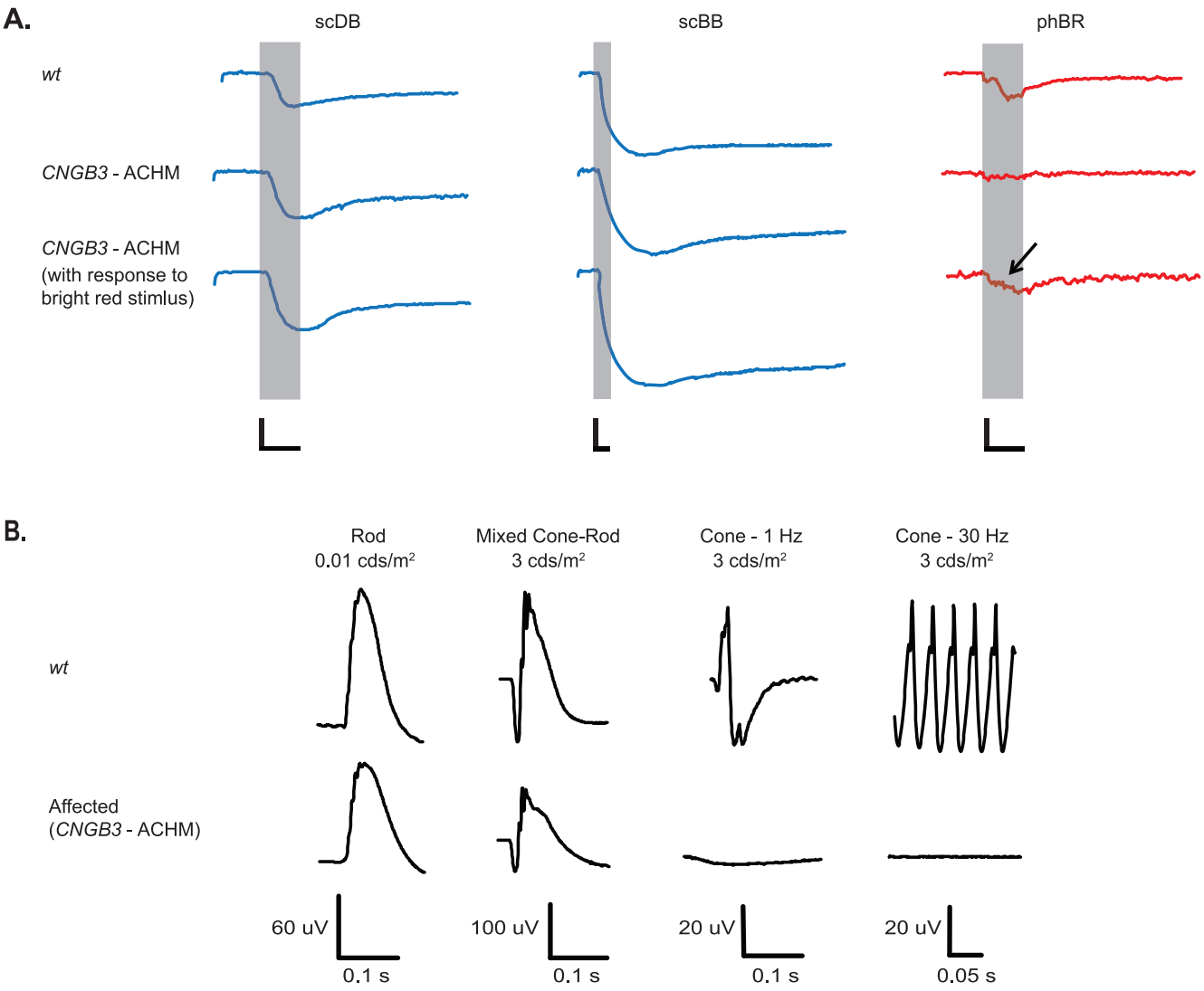

Figure 3. (**A**) PLRs from dogs carrying the *CNGB3* mutation with ACHM with the expected abrogation of phBR responses. In contrast, a subset of *CNGB3*-mutants with incomplete ACHM showed persistent but reduced phBR responses (*arrow*). Representative recordings are shown here. Recordings from all dogs are shown in Supplementary Figure S3. *Shaded area* represents the 1-s light stimulus presentation. (**B**) Comparison of representative full-field ERGs recorded from CNGB3 mutants show normal rod-mediated function but lost cone-mediated function compared to WT dogs. (**A**) *Calibration bars*: 1 s (time, *horizontal*) and 20% (normalized pupil size, *vertical*).

to 10 individual clones were sequenced using Automated 3730 DNA analyzer (Applied Biosystems), aligned to the predicted sequence (CanFam 2.0 assembly; http://genome.ucsc.edu/cgi-bin/hgGateway, in the public domain) using Sequencher version 4.2.2 software (Gene Codes Corp., Ann Arbor, MI, USA), and submitted to GeneBank (accession number KU341721). The predicted amino acid sequence of the canine melanopsin was aligned with those of other species by using Clustal Omega software (http://www.ebi.ac.uk/Tools/msa/, in the public domain).

qRT-PCR Analysis of Retinal Gene Expression

Primers and TaqMan Probes were designed for canine melanopsin/*Opn4* using Primer Express software version 2.0 (Applied Biosystems). Primer pair and probe were designed to neighboring exon sequences to ensure that only cDNA and not genomic DNA was amplified. Using cDNA synthesized as described above, qRT-PCR was performed with the custom-designed primer pairs MelDegE67F (forward, GCGGCTACAGA GAGAGTGGAA) and MelDegE67R (reverse, ACATGA ACTCCGTGCCAGC) and probe (CTTTCGCTGGGTATT) that spans the junction of exons 6 and 7. All qRT-PCR assays were performed in 96-well plates using 7500 model real-time PCR machine with 7500 v2.0.1 detection software (Applied Biosystems).

Relative melanopsin/*Opn4* gene expression was compared with that of the *GAPDH* product and calculated as [1/(2^{$Ct_{Gene} - Ct_{GAPDH}$})]. The ratios of relative gene expression were calculated between the diseased eye and age-matched WT control, using the ΔΔCT method.[41] Ratios different from 1 were considered relevant, indicating either increased (>1) or decreased (<1) gene expression.

Immunohistochemistry

Retinal IHC was performed as previously described.[41–43] Immunohistochemical staining was performed using the antibodies shown in Supplementary Table S3. A custom-made rabbit anti-canine melanopsin antibody directed at a mixture of

Investigative Ophthalmology & Visual Science

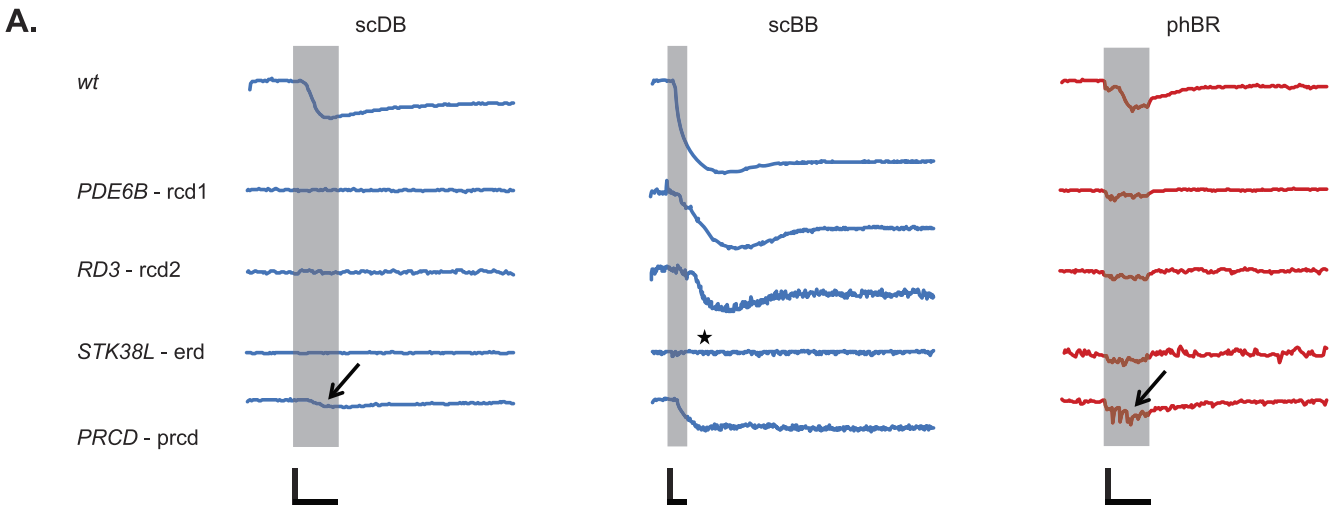

Figure 4. (**A**) Representative PLRs of older dogs bearing mutations in *PDE6B*, *RD3*, *STK38L*, and *PRCD*. Recordings from all dogs with mutations in *STK38L*, *IQCB1*, *RPGR*, *RPE65*, and *PRCD* and older dogs carrying *PDE6B*, *RD3*, and *PDE6A*-mutations are shown in Supplementary Figure S4. *Shaded area* represents the 1-s light stimulus presentation. ★ indicates absent PLR to scBB in one older *STK38L*-mutant. *Arrows* indicate small residual rod function and near-normal preserved cone function in an older dog with mutated PRCD. (**B**) Representative full-field ERGs recorded from older dogs bearing mutations in *PDE6B*, *STK38L*, and *PRCD*. Responses of a WT dog are shown for comparison. For *PDE6B*- and *STK38K*-mutant dogs, rod- and cone- mediated function was non-recordable. For the *PRCD*-mutant dog, cone-mediated function was recordable, but the amplitude was reduced compared with that of the WT dog. (**A**) *Calibration bars*: 1 s (time, *horizontal*) and 20% (normalized pupil size, *vertical*).

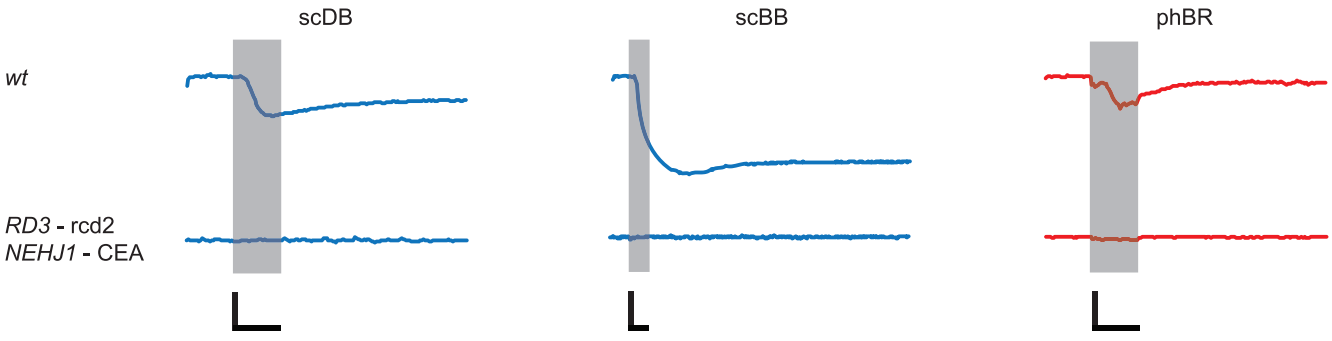

Figure 5. All PLRs were absent in the dog affected by a mutation in *RD3* and concurrent severe optic nerve head coloboma due to a mutation in *NEHJ1*. *Shaded area* indicates the 1-s light stimulus presentation. *Calibration bars*: 1 s (time, *horizontal*) and 20% (normalized pupil size, *vertical*).

Investigative Ophthalmology & Visual Science

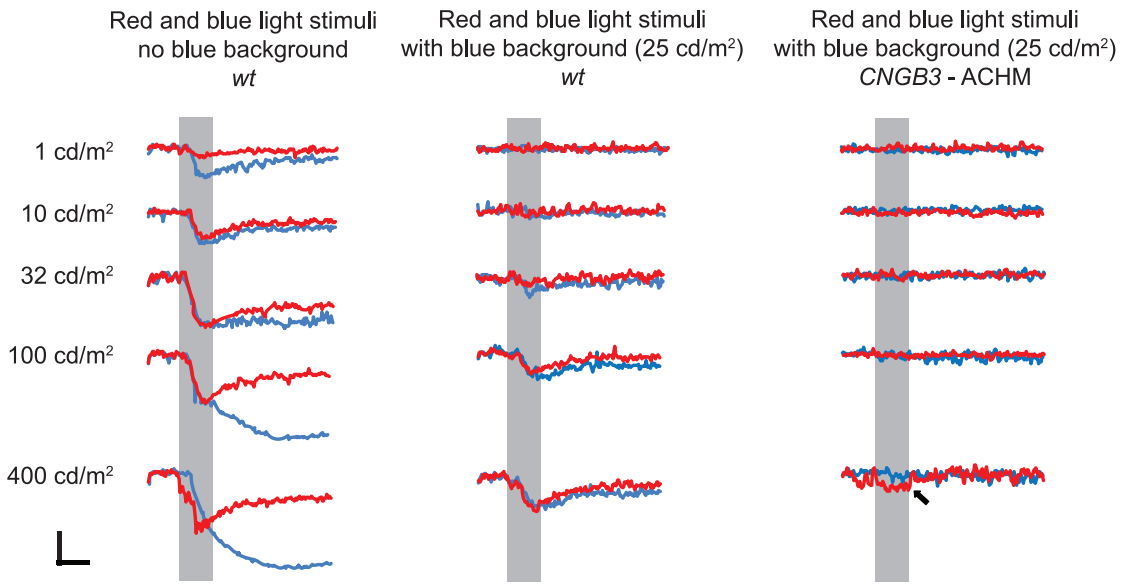

Figure 6. Results of PLR testing in scotopic and photopic light intensity series. Average PLRs for the 2 WT dogs to photopically matched red and blue light at five intensity levels are shown (*left* and *middle* columns). Results of photopic light intensity series testing in 2 dogs with *CNGB3* mutation (*right column*). Average PLRs for the affected dogs to the red and blue light at five intensity levels are shown. *Arrow* indicates light artifact noted at high red light intensity (400 cd/m^2) with 25 cd/m^2 blue background. For all graphs, *shaded areas* indicate 1-s light stimulus presentation. *Calibration bars*: 1 s (time, *horizontal*) and 20% (normalized pupil size, *vertical*).

N-terminal (NH_2-MNPPSGPGAQEPGC-amide) and C-terminal (CAKAPLRPRGQAVETPGKV-amide) peptides (21st Century Biochemicals, Marlboro, MA, USA) was generated and affinity purified. Alexa Fluor-labeled chicken anti-rabbit immunoglobulin G (IgG), goat anti-rabbit IgG, or goat anti-mouse IgG was used as secondary antibody. 4′,6-Diamidino-2-phenylindole (DAPI) stain was used to detect cell nuclei. Slides were mounted using Gelvatol (Sigma-Aldrich Corp., St. Louis, MO, USA) and were imaged using a FluoView FV1000 confocal laser scanning microscope (Olympus America, Inc, Center Valley, PA, USA).

Results

Normal Chromatic Pupillometry Recorded From WT Dogs

We assessed pupillary responses in 5 WT dogs, using testing parameters developed based on a human protocol (Fig. 1).[10] After a 10-min dark adaptation, mean pupil diameter was 10.8 ± 2.4 mm. Mean ± SD percentage of constriction amplitudes induced by scDB, scBB, and phBR stimuli in WT dogs were 21.3% ± 10.6%, 50.0% ± 17.5%, and 19.4% ± 7.4%, respectively. Mean latencies of PLRs elicited by scDB, scBB, and phBR stimuli in WT dogs were 0.26 ± 0.05 s, 0.28 ± 0.10 s, and 0.32 ± 0.03 s, respectively. The PLRs to the scBB stimuli were characterized by a sustained response (7.7 ± 4.6 min after the offset of the stimulus), which is thought to be melanopsin-driven.[5,10] A small light artifact (movement of the pupil detector) was observed for several milliseconds after onset of the phBR light stimulus.

Individual dogs exhibited considerable variation in pupil constriction amplitudes (Fig. 1A), which was significantly correlated with baseline pupil size for scBB ($r = 0.72$, $P < 0.05$), but not for scDB ($r = 0.46$; $P = 0.19$) or phBR ($r = –0.27$; $P = 0.45$) stimuli (Fig. 1B). No other obvious cause for this variation was evident, including age, sex, or anesthesia level.

Primary Rod Disease Results in Absence of Pupillary Responses to scDB

Chromatic pupillometry results concurred with prior descriptions of functional phenotype of the respective diseases. In contrast with WT dogs, young dogs with *PDE6A*-rcd3 and *PDE6B*-rcd1, and dogs with *CNGB1*-PRA exhibited no measurable PLRs to scDB used to test rod function (Fig. 2, Supplementary Fig. S2). A sustained response was elicited by scBB, which represents the melanopsin-driven response,[5,10] and persisted in all affected dogs.

As expected, based on known disease phenotypes, phBR evoked measurable PLRs in most of the affected dogs and were likely cone-mediated. In one of the younger (0.4-year-old) *PDE6B*-mutant dogs, ERG was recorded during the same session as chromatic pupillometry and showed an absence of rod-mediated response but preservation of reduced cone responses (Fig. 2B). Unexpectedly, no recordable responses to phBR were present in the *PDE6A*- and both *CNGB1*-mutant dogs as confirmed by video observation. It is possible that small cone responses were present, as shown in the ERG of the *PDE6A* mutant dog (Fig. 2B), but were overshadowed by the light artifact.

The mean constriction amplitude induced by scBB for all affected dogs (49.1% ± 13.4%) and phBR for mutant dogs excluding nonresponders (24.2% ± 23.6%) were unaltered with respect to those seen in WT dogs ($P = 0.89$ and $P = 0.55$, respectively). The mean latencies of responses to scBB and phBR in mutant dogs were likewise unaltered with respect to those seen in WT dogs (0.32 ± 9.56 s; $P = 0.37$; and 0.27 ± 9.32 s; $P = 0.89$, respectively).

Variations in pupil constriction amplitude were noted between individual *PDE6B*-mutant dogs (Supplementary Fig. S2), as we likewise found in WT dogs that were not attributable to differences in age, sex, or anesthesia levels. Constriction amplitudes evoked by scBB ($P = 0.14$) or phBR ($P = 0.84$) testing protocols were not significantly correlated with baseline pupil size.

Primary Cone Disease Reduces Pupil Responses to phBR

In 4 of 6 *CNGB3*-mutants, response to phBR was absent, except for the light artifact (Fig. 3A, Supplementary Fig. S3), supporting the notion that this stimulus specifically elicits cone-mediated PLRs. Responses to both scDB and scBB were well preserved. The results of chromatic pupillometry corresponded with the ERGs, as rod function was normal but cone function was lost in dogs with *CNGB3*-ACHM (Fig. 3B). Although most chromatic pupillometry results showed loss of cone function as expected based on prior phenotypic descriptions, the remaining 2 of 6 *CNGB3*-mutant dogs (3CNGB3 and 5CNGB3 dogs) did exhibit persistent pupillary responses to phBR (Fig. 3A, arrow), consistent with incomplete ACHM (Koehl K, et al. *IOVS* 2015;56:ARVO E-Abstract 4651). Their mean constriction amplitudes were markedly reduced compared with that in WT dogs (9.1% ± 2.4% vs. 19.4% ± 7.4%, respectively). Mean latency of response to phBR was similar to that seen in WT dogs (0.26 ± 0.05 s). Sample size ($n = 2$) in this *CNGB3*-subset did not permit statistical analysis.

The mean pupil constriction amplitudes evoked by the scDB were significantly greater (31.2% ± 6.2%; $P = 0.02$) than that seen in WT dogs (21.3% ± 10.6%), but those to scBB were similar (63.4% ± 8.7%; $P = 0.16$). Mean latency of responses to scDB (0.29 ± 0.06 s) and scBB (0.27 ± 0.07s; $P = 0.78$) were unaltered compared with those in WT dogs ($P = 0.26$ and $P = 0.78$, respectively). Comparable to WT dogs, individual *CNGB3* mutants exhibited variations in pupil constriction amplitude that were not attributable to age, sex, or anesthesia level (Supplementary Fig. S3). We found a significant positive correlation between baseline pupil size and constriction amplitude for scBB ($r = 0.72$; $P < 0.05$) but not for scDB ($r = –0.34$; $P = 0.34$).

Response to scBB Persists in Advanced Outer Retinal Diseases

With advanced retinal disease due to various vision-impairing mutations, pupillary responses to scDB and phBR were reduced or absent, consistent with progressive loss of rod and cone function (Fig. 4A, Supplementary Fig. S4). With one exception (see below), the response to scBB was maintained in all dogs, even when rod- and cone-mediated retinal functions were not detectable, providing strong evidence that this stimulus is specific for inner retina. Mean PLR latency was approximately doubled in these dogs (0.61 ± 0.26 s vs. 0.28 ± 0.10 s, respectively) by 0.33 s compared to that in WT dogs ($P = 0.0003$), consistent with a melanopsin-mediated pupillary response without rod or cone influence.[44] The scBB-evoked mean constriction amplitude was significantly decreased by 11.7% compared to that in WT dogs (38.3% ± 13.9% vs. 50.0% ± 17.5%, respectively; $P = 0.03$), indicating loss of contribution of rods and cones to the initial constriction amplitude.[44]

One of the older prcd-affected dogs had both rod and cone function preserved, evident in responses seen both by chromatic pupillometry and ERG (Fig. 4). In an older *STK38L*-mutant, PLR to all light stimuli, including scBB, was absent. Such loss of inner retinal response is due to advanced retinal degeneration also involving the inner retina (see Presence of ipRGC and Melanopsin Expression in Diseased Retinas below),[36,45] as the function of STK38L is not known to impact inner retinal responses.

Variations in pupil constriction amplitude were also noted between individual mutant dogs (Supplementary Fig. S4), as in WT dogs, which was not attributable to age, sex, or anesthesia level but potentially could result from individual variations in disease severity. Baseline pupil size was not significantly correlated with constriction amplitudes seen with scBB ($P = 0.14$) or phBR ($P = 0.43$).

Loss of ipRGC Function

The dog with severe optic nerve head coloboma associated with *NEHJ1* mutation was also affected with *RD3* rcd2. As expected, all pupillary responses were absent, including response to scBB (Fig. 5).

Variations in Constriction Amplitude: Reproducibility and Light Intensity Series

Three dogs (1 WT and 2 *CNGB3*-mutants with incomplete ACHM) were retested twice within 4 to 5 months. We found that recorded PLRs were highly reproducible, supporting the diagnostic value of chromatic pupillometry in dogs (Supplementary Fig. S5).

We hypothesized that the individual variations in constriction amplitudes seen between WT dogs could have been due to differences in entrance pupil size, and hence, amount of light entering the eyes. To test this idea and assess the role of light stimulus intensity on pupil responses under scotopic and photopic conditions, we tested responses to a light intensity series in 2 WT dogs and found that stimulus intensity and constriction amplitude are related (Fig. 6).

Under scotopic conditions (Fig. 6, left column), saturation of peak amplitudes occurred at high light intensities (32–400 cd/m^2) and recovered rapidly with the red light stimuli, whereas PLRs to the photopically matched blue stimuli were characterized by a sustained postillumination response for intensities ≥32 cd/m^2, which we attribute to melanopsin-driven response.[5] Contrasting with PLRs under scotopic conditions, under photopic conditions with a blue background light of 25 cd/m^2 (Fig. 6, middle column), PLRs to red stimuli were fairly similar to PLRs seen in photopically matched blue stimuli, presumably both were cone-mediated. No sustained response was seen to blue stimuli under photopic conditions, suggesting that the blue background suppressed ipRGC activity. A light artifact was noted for approximately 0.1 s after red and blue stimuli onset at high light intensities (100 and 400 cd/m^2, respectively). In addition to the WT dogs, 2 *CNGB3* mutants were tested under photopic conditions to determine the stimulus intensity at which light artifacts occur. PLRs were absent in all blue and red light stimuli. A small light artifact was only noted at a high red light intensity of 400 cd/m^2 (Fig. 6, right column).

Presence of ipRGC and Melanopsin Expression in Diseased Retinas

To permit melanopsin quantification and analyses in dogs by enabling design of antibodies and qRT-PCR primers, we cloned the canine melanopsin/*Opn4* gene. The full-length cDNA contains a 1,446-bp open reading frame encoding a 482-amino acid protein (Supplementary Fig. S6). Alignment of the isolated canine amino acid sequence with those of mouse, chicken, lizard, and human melanopsin revealed substantial homologies. The highest sequence similarity (89.6%) was with the cat homolog, whereas weaker similarity (46.63%) was evident with the Italian wall lizard homolog. Dog melanopsin showed approximately 75.4% amino acid sequence similarity to that of mouse and rat homologs and approximately 78.9% to that of human homolog.

Using qRT-PCR, we observed a significant decrease in melanopsin/*Opn4* expression in advanced stages of prcd compared to that in age-matched WT dogs ($P < 0.05$) (Fig. 7A). Melanopsin/*Opn4* expression levels in early onset retinal

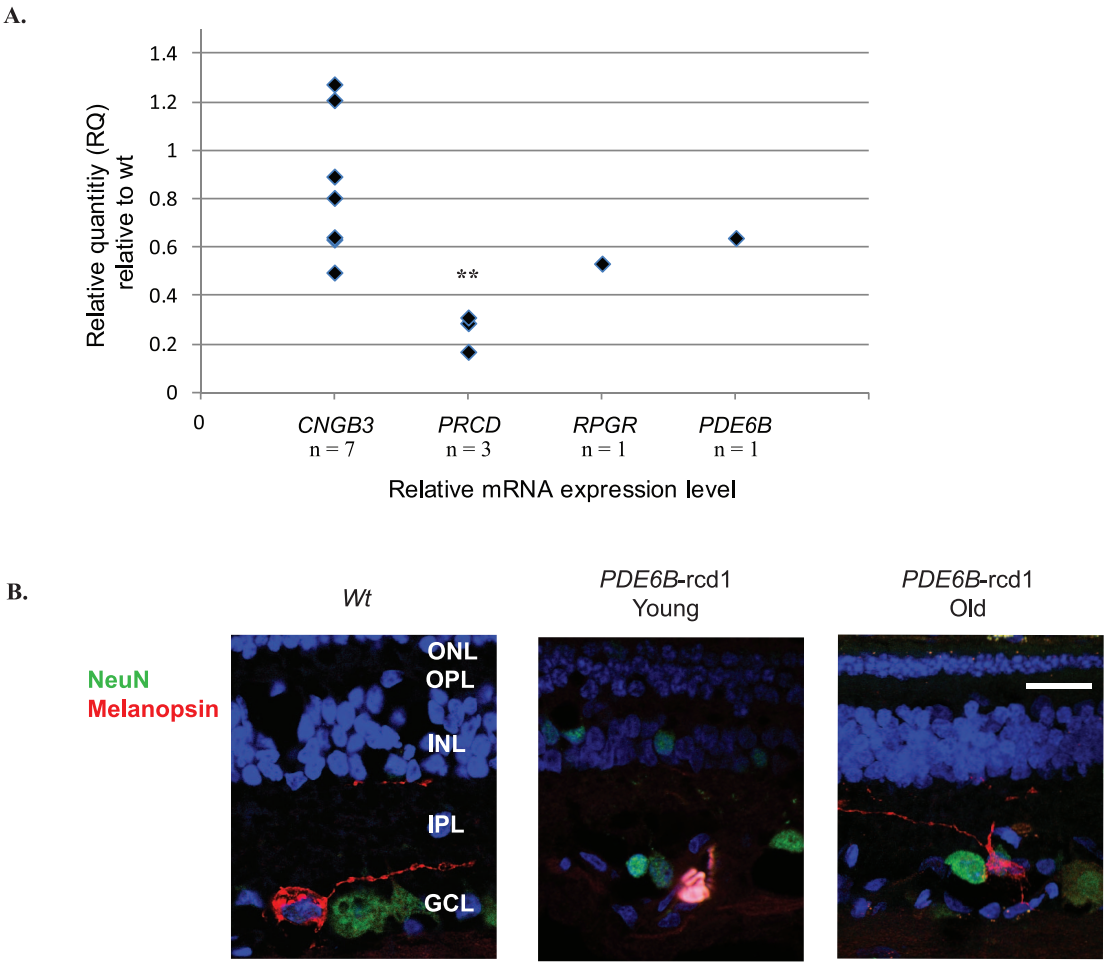

Figure 7. Gene and protein expression patterns in dogs with inherited retinal diseases compared to those in WT dogs. (**A**) Effects of inherited retinal disease in various canine models on retinal melanopsin/*Opn4* mRNA expression levels, quantified by qRT-PCR and compared with those in age-matched WT dogs. Melanopsin/*Opn4* was variable but not significantly altered in *CNGB3*-ACHM. Retinas in *PRCD*-mutants showed a significant decrease (**) compare with those in WT retinas ($P < 0.05$). Expression levels in individual *RPGR*- and *PDE6B*-mutants also appeared decreased. (**B**) Melanopsin immunostaining of representative retinal sections from WT and *PDE6B*-mutant dogs confirms the presence of ipRGCs. Other RGCs are shown in *green* (NeuN). Cell nuclei are shown in *blue* with DAPI staining. *Calibration bar*: 20 μm. GCL, ganglion cell layer; INL, inner nuclear layer; IPL, inner plexiform layer; ONL, outer nuclear layer; OPL, outer plexiform layer.

degeneration in *RPGR*- and *PDE6B*-mutant dogs was also decreased, but this finding was inconclusive due to small sample sizes. In contrast, melanopsin/*Opn4* expression was variable but not significantly altered in *CNGB3*-mutant dogs with ACHM, a nondegenerative retinal disease ($P = 0.193$). Melanopsin immunostaining of representative retinal sections confirmed the presence of melanopsin-expressing ipRGCs in WT and young and old *PDE6B*-mutant dogs, consistent with positive PLRs to scBB (Fig. 7B).

Immunolabelling of representative retinal sections confirmed the previously reported histologic phenotype of the studied diseases, including the preservation of RGCs in most affected dogs (Supplementary Fig. S7). In contrast, an *STK38L*-mutant dog (1erd) showed loss of normal retinal architecture by IHC,[36,41,45] with complete loss of RGCs due to severe retinal degeneration, thus accounting for the observed absence of any scBB response.

Discussion

Our findings validate the use of an available human chromatic pupillometry clinical testing protocol for dogs.[10] The evaluation of a previously established human protocol was justified by the fact that the absorption spectra of canine photoreceptors are similar to those in humans (Supplementary Table S4). Standard pupillometry has been used in dogs before, and chromatic pupillometry has been suggested, but we have now confirmed the validity of this method in this species.[11–13,46–48]

By taking advantage of purpose-bred dogs with well-defined retinal disease phenotypes, we verified that pupil constriction evaluated in the dark by dim and bright blue light is specific for rod and ipRGC functions, respectively, and that a bright red light stimulus on a blue-lit background is specific for cone function. For example, we found that young dogs affected by *PDE6B*-rcd1, which are expected to have a complete lack of rod function with initially intact cone function, exhibited no PLR response to scDB.

As reported previously in humans, in dogs a blue background used in the cone protocol also suppresses rod and ipRGC responses, allowing the testing of cones.[10,49] Based on the known absorbance spectrum of canine cone opsins, the phBR protocol selectively favors testing of long- and medium-wavelength-absorbing (L/M) cones. We validated this cone protocol by testing dogs with decreased or lost cone function, such as in *CNGB3*-ACHM. In humans, a unique feature of

complete ACHM is paradoxical pupillary constriction in darkness,[50–52] seen when a patient is moved to darkness after exposure to bright light for several minutes. However, we did not observe paradoxical pupil constriction in our *CNGB3*-ACHM dogs. Whether this was due to species difference or other reasons remains to be determined.

We found that a bright blue light stimulus successfully isolated ipRGC function. This response was well preserved unless inner retina and optic nerve were impaired, as seen in dogs affected with severe optic nerve head coloboma or advanced retinal degeneration. The complete loss of RGCs seen by IHC in one *STK38L*-mutant dog corresponded with the absence of its response to scBB. This finding suggests that, in the future, ipRGC response testing may be exploited to quantify optic nerve damage by determining the extent to which the scBB response correlates with the number of viable optic nerve axons.

Only blue light of intensities $\geq$32 cd/m^2 evoked sustained postillumination pupil responses in dogs; these exceed those reported in humans (10 cd/m^2).[10] Such sustained responses are thought to be melanopsin-driven.[5,6,8] In macaques, for example, after pharmacologic blockade of the classic rod and cone photoreceptors, the melanopsin-driven pupillary responses persisted after light stimulus offset.[5] This sustained response has been defined as postillumination pupil response (PIPR).[53] Recent studies have used PIPR to assess the function of the melanopsin signaling pathway and to measure disease-related progressive changes in ipRGC function.[53–57] In patients with advanced glaucoma, the PIPR was reduced compared to that in normal age-matched patients.[54,55] Also, redilation time was found to be slower for patients lacking rods or cones.[44] We observed a sustained PIPR in all dogs that had intact inner retinas. Because the pupillometry system recorded only to 14 s after light offset, we were unable to calculate the full extent of PIPR.[53,54]

Our findings in ipRGC testing revealed interesting effects upon PLR latency in dogs with losses of rod and cone function. Latency of the PLR response for scBB in dogs with selective loss of either rod or cone function was unaltered with respect to that of WT dogs, but detectable PLR latencies were significantly prolonged in dogs with combined loss of both rod and cone functions. The rapid pupillary constriction evoked by light stimulus onset is mediated by rods and cones.[44] Accordingly, as found in human studies,[44] onset of pupil responses in affected dogs lacking both rod and cones was abnormally slow, as expected if mediated purely by melanopsin, which has long latency.

Our findings also provide the first demonstration of melanopsin/*Opn4*-expressing ipRGCs in the normal and diseased canine retina. Melanopsin/*Opn4* mRNA expression was decreased in a canine model of late-onset retinal degeneration but was unchanged in non-degenerative retinal disease such as ACHM.

Although our findings strongly support the prospects for using chromatic pupillometry as an additional diagnostic tool for testing of canine outer and inner retinal function, the current testing protocol still needs to be optimized, and there are limitations to this study. Most importantly, improvements are needed in the Roland system to eliminate the artifact noted with phBR light stimulation for the cone-testing protocol to eliminate the red light artifact, which impedes the ability to detect very small responses. This may account for the absence of detectable cone response in a young *PDE6A*-mutant dog. It is possible that the stopband filter (λ_s) of 700 nm for the infrared camera in the Ganzfeld dome was not high enough to prevent light admission from the 640-nm red LED, causing a light artifact. Due to the light artifact, we found that it was important to observe the real-time video recording of the phBR light testing with blue background, to determine if there was a true pupil response.

Although we found good test-retest reproducibility for individual dogs, there was considerable variation in constriction amplitudes between dogs, which may prevent interpretations about the numbers of photosensitive cells. Although pupillometry is an objective means for precise quantitative measurement of changes in pupil size, certain factors can affect pupil size and contraction, including retinal illumination, accommodative state of the eye, age, and emotional conditions.[58–61] Important sources of such variability, confirmed by our results, are differences in baseline pupil size and amount of retinal illumination. Kardon et al.[62] determined in eyes with darkly pigmented irides that baseline pupil size strongly influence retinal illumination. Such variability could also be due to mechanical effects of small pupil size on iris movement.[63] We used a closed-loop paradigm, such that PLR was measured in the same eye that received the light stimulation; hence, retinal illumination was affected by baseline pupil size. To minimize the influence of pupil size, an open-loop paradigm could be used in which one pupil is dilated pharmacologically and stimulated with light but recordings are taken from the undilated contralateral eye.

Another potential cause of such variability may be anesthesia level and anesthetic drug used, but by monitoring relevant variables measured on our dogs during anesthesia, including heart rate and blood pressure, we found that these variables were very consistent, showing little variability. Significant differences in pupillometry parameters have been reported in humans treated with different anesthetics.[64] The medications used for anesthesia in that particular study, ketamine and xylazine, reportedly elicit mydriatic effects in dogs. The anesthetics we used were acepromazine, propofol, and isoflurane. Administration of acepromazine in dogs has been shown to cause miosis, and halogenated agents (isoflurane) cause mydriasis, whereas propofol does not alter pupil reactivity.[65,66] Despite these reported effects of anesthetic agents on the pupil, we found that the dogs' eyes dilated well to baseline pupil size after dark adaptation.

Further research work is needed to define conditions that minimize individual variability in pupil constriction amplitude. As handheld pupillometry devices become more readily available, it will be possible in the future to eliminate use of anesthetic agents for PLR testing. With a handheld device, anesthesia and head positioning in the Ganzfeld dome would be less critical, allowing easy performance of chromatic pupillometry, and perhaps decreasing the individual variability of pupil constriction. A recent study found that the handheld pupillometer was easy to use on dogs, and its use was equally facile in conscious and anesthetized dogs.[64]

Conclusions

In summary, we validated the use of a chromatic pupillometry protocol in dogs to assess rod, cone, and ipRGC function. We found that chromatic pupillometry results in dogs with specific retinal diseases correlated well with the known disease phenotype, including ERG, IHC, and qRT-PCR results. These findings are translationally relevant, as dogs have become increasingly important for the research of inherited retinal diseases and development of novel therapies.[14,67] For example, our pupillometry approach may assist evaluation of the outcome of retinal gene therapy by complementing ERG recordings and visual behavioral testing to enable complete functional assessment of retinal and central visual pathways.[49,68–74]

Investigative Ophthalmology & Visual Science

Acknowledgments

The authors thank Gustavo D. Aguirre and William A. Beltran for the use of the animals at the Retinal Disease Study Facility, University of Pennsylvania; Karina E. Guziewicz for assistance in primer design; Melinda Frame, Michigan State University, for assistance with confocal microscopy; Cheryl Craft, University of Southern California, for the hCAR antibody; and the staff at the RDSF, University of Pennsylvania, and Gabriel A. Stewart, Michigan State University, for technical support.

Supported by U.S. National Institutes of Health Grants EY-019304, 017549, 006855, and T32-RR007063; Department of Veterans Affairs Rehabilitation, Research, and Development Division Grant C9251-C; the Foundation Fighting Blindness, the Michigan State University College of Veterinary Medicine Endowed Research Funds, and the Gary L. Blanchard Fund.

Disclosure: **C.Y. Yeh**, None; **K.L. Koehl**, None; **C.D. Harman**, None; **S. Iwabe**, None; **J.M. Guzman**, None; **S.M. Petersen-Jones**, None; **R.H. Kardon**, MedFace LLC (S), Face X LLC (S), Novartis (C), P; **A.M. Komáromy**, None

References

1. Berson DM, Dunn FA, Takao M. Phototransduction by retinal ganglion cells that set the circadian clock. *Science*. 2002;295:1070–1073.
2. Hattar S, Liao HW, Takao M, Berson DM, Yau KW. Melanopsin-containing retinal ganglion cells: architecture, projections, and intrinsic photosensitivity. *Science*. 2002;295:1065–1070.
3. Hattar S, Lucas RJ, Mrosovsky N, et al. Melanopsin and rod-cone photoreceptive systems account for all major accessory visual functions in mice. *Nature*. 2003;424:76–81.
4. Guler AD, Ecker JL, Lall GS, et al. Melanopsin cells are the principal conduits for rod-cone input to non-image-forming vision. *Nature*. 2008;453:102–105.
5. Gamlin PD, McDougal DH, Pokorny J, Smith VC, Yau KW, Dacey DM. Human and macaque pupil responses driven by melanopsin-containing retinal ganglion cells. *Vision Res*. 2007;47:946–954.
6. Dacey DM, Liao HW, Peterson BB, et al. Melanopsin-expressing ganglion cells in primate retina signal colour and irradiance and project to the LGN. *Nature*. 2005;433:749–754.
7. Provencio I, Rodriguez IR, Jiang G, Hayes WP, Moreira EF, Rollag MD. A novel human opsin in the inner retina. *J Neurosci*. 2000;20:600–605.
8. Kardon R, Anderson SC, Damarjian TG, Grace EM, Stone E, Kawasaki A. Chromatic pupil responses: preferential activation of the melanopsin-mediated versus outer photoreceptor-mediated pupil light reflex. *Ophthalmology*. 2009;116:1564–1573.
9. Kardon R, Anderson SC, Damarjian TG, Grace EM, Stone E, Kawasaki A. Chromatic pupillometry in patients with retinitis pigmentosa. *Ophthalmology*. 2011;118:376–381.
10. Park JC, Moura AL, Raza AS, Rhee DW, Kardon RH, Hood DC. Toward a clinical protocol for assessing rod, cone, and melanopsin contributions to the human pupil response. *Invest Ophthalmol Vis Sci*. 2011;52:6624–6635.
11. Grozdanic SD, Matic M, Sakaguchi DS, Kardon RH. Evaluation of retinal status using chromatic pupil light reflex activity in healthy and diseased canine eyes. *Invest Ophthalmol Vis Sci*. 2007;48:5178–5183.
12. Whiting RE, Yao G, Narfstrom K, et al. Quantitative assessment of the canine pupillary light reflex. *Invest Ophthalmol Vis Sci*. 2013;54:5432–5440.
13. Grozdanic SD, Kecova H, Lazic T. Rapid diagnosis of retina and optic nerve abnormalities in canine patients with and without cataracts using chromatic pupil light reflex testing. *Vet Ophthalmol*. 2013;16:329–340.
14. Petersen-Jones SM, Komaromy AM. Dog models for blinding inherited retinal dystrophies. *Hum Gene Ther Clin Dev*. 2015;26:15–26.
15. Gelatt KN, Brooks DE, Samuelson DA. Comparative glaucomatology. I: The spontaneous glaucomas. *J Glaucoma*. 1998;7:187–201.
16. Suber ML, Pittler SJ, Qin N, et al. Irish setter dogs affected with rod/cone dysplasia contain a nonsense mutation in the rod cGMP phosphodiesterase beta-subunit gene. *Proc Natl Acad Sci U S A*. 1993;90:3968–3972.
17. Zhang Q, Acland GM, Wu WX, et al. Different *RPGR* exon ORF15 mutations in Canids provide insights into photoreceptor cell degeneration. *Hum Mol Genet*. 2002;11:993–1003.
18. Goldstein O, Kukekova AV, Aguirre GD, Acland GM. Exonic SINE insertion in *STK38L* causes canine early retinal degeneration (ERD). *Genomics*. 2010;96:362–368.
19. Zangerl B, Goldstein O, Philp AR, et al. Identical mutation in a novel retinal gene causes progressive rod-cone degeneration in dogs and retinitis pigmentosa in humans. *Genomics*. 2006;88:551–563.
20. Sidjanin DJ, Lowe JK, McElwee JL, et al. Canine *CNGB3* mutations establish cone degeneration as orthologous to the human achromatopsia locus ACHM3. *Hum Mol Genet*. 2002;11:1823–1833.
21. Ahonen SJ, Arumilli M, Lohi H. A *CNGB1* frameshift mutation in Papillon and Phalene dogs with progressive retinal atrophy. *PLoS One*. 2013;8:e72122.
22. Winkler PA, Ekenstedt KJ, Occelli LM, et al. A large animal model for *CNGB1* autosomal recessive retinitis pigmentosa. *PLoS One*. 2013;8:e72229.
23. Kukekova AV, Goldstein O, Johnson JL, et al. Canine *RD3* mutation establishes rod–cone dysplasia type 2 (rcd2) as ortholog of human and murine rd3. *Mamm Genome*. 2009;20:109–123.
24. Chader GJ, Fletcher RT, Sanyal S, Aguirre GD. A review of the role of cyclic GMP in neurological mutants with photoreceptor dysplasia. *Curr Eye Res*. 1985;4:811–819.
25. Santos-Anderson RM, Tso MO, Wolf ED. An inherited retinopathy in collies. A light and electron microscopic study. *Invest Ophthalmol Vis Sci*. 1980;19:1281–1294.
26. Woodford BJ, Liu Y, Fletcher RT, et al. Cyclic nucleotide metabolism in inherited retinopathy in collies: a biochemical and histochemical study. *Exp Eye Res*. 1982;34:703–714.
27. Petersen-Jones SM, Entz DD, Sargan DR. cGMP phosphodiesterase-alpha mutation causes progressive retinal atrophy in the Cardigan Welsh corgi dog. *Invest Ophthalmol Vis Sci*. 1999;40:1637–1644.
28. Keep JM. Clinical aspects of progressive retinal atrophy in the Cardigan Welsh Corgi. *Aust Veterinary J*. 1972;48:197–199.
29. Aguirre GD, Baldwin V, Pearce-Kelling S, Narfstrom K, Ray K, Acland GM. Congenital stationary night blindness in the dog: common mutation in the *RPE65* gene indicates founder effect. *Mol Vis*. 1998;4:23.
30. Veske A, Nilsson SE, Narfstrom K, Gal A. Retinal dystrophy of Swedish briard/briard-beagle dogs is due to a 4-bp deletion in *RPE65*. *Genomics*. 1999;57:57–61.
31. Nilsson SE, Wrigstad A, Narfstrom K. Changes in the DC electroretinogram in Briard dogs with hereditary congenital night blindness and partial day blindness. *Exp Eye Res*. 1992;54:291–296.
32. Wrigstad A, Nilsson SE, Narfstrom K. Ultrastructural changes of the retina and the retinal pigment epithelium in Briard dogs with hereditary congenital night blindness and partial day blindness. *Exp Eye Res*. 1992;55:805–818.

Investigative Ophthalmology & Visual Science

33. Kijas JW, Zangerl B, Miller B, et al. Cloning of the canine *ABCA4* gene and evaluation in canine cone-rod dystrophies and progressive retinal atrophies. *Mol Vis*. 2004;10:223–232.
34. Goldstein O, Mezey JG, Schweitzer PA, et al. *IQCB1* and *PDE6B* mutations cause similar early onset retinal degenerations in two closely related terrier dog breeds. *Invest Ophthalmol Vis Sci*. 2013;54:7005–7019.
35. Beltran WA, Hammond P, Acland GM, Aguirre GD. A frameshift mutation in RPGR exon ORF15 causes photoreceptor degeneration and inner retina remodeling in a model of X-linked retinitis pigmentosa. *Invest Ophthalmol Vis Sci*. 2006;47:1669–1681.
36. Acland GM, Aguirre GD. Retinal degenerations in the dog: IV. Early retinal degeneration (erd) in Norwegian elkhounds. *Exp Eye Res*. 1987;44:491–521.
37. Parker HG, Kukekova AV, Akey DT, et al. Breed relationships facilitate fine-mapping studies: a 7.8-kb deletion cosegregates with Collie eye anomaly across multiple dog breeds. *Genome Res*. 2007;17:1562–1571.
38. Aguirre GD, Rubin LF. Rod-cone dysplasia (progressive retinal atrophy) in Irish setters. *J Am Vet Med Assoc*. 1975;166:157–164.
39. Parry HB. Degenerations of the dog retina. VI. Central progressive atrophy with pigment epithelial dystrophy. *Br J Ophthalmol*. 1954;38:653–668.
40. Bergamin O, Kardon RH. Latency of the pupil light reflex: sample rate, stimulus intensity, and variation in normal subjects. *Invest Ophthalmol Vis Sci*. 2003;44:1546–1554.
41. Berta AI, Boesze-Battaglia K, Genini S, et al. Photoreceptor cell death, proliferation and formation of hybrid rod/S-cone photoreceptors in the degenerating *STK38L* mutant retina. *PLoS One*. 2011;6:e24074.
42. Komaromy AM, Rowlan JS, Corr AT, et al. Transient photoreceptor deconstruction by CNTF enhances rAAV-mediated cone functional rescue in late stage *CNGB3*-achromatopsia. *Mol Ther*. 2013;21:1131–1141.
43. Beltran WA, Boye SL, Boye SE, et al. rAAV2/5 gene-targeting to rods: dose-dependent efficiency and complications associated with different promoters. *Gene Ther*. 2010;17:1162–1174.
44. Gooley JJ, Ho Mien I, St Hilaire MA, et al. Melanopsin and rod-cone photoreceptors play different roles in mediating pupillary light responses during exposure to continuous light in humans. *J Neurosci*. 2012;32:14242–14253.
45. Gelatt KN, Gilger BC, Kern TJ. Veterinary Ophthalmology. 5th ed. Ames, Iowa: Wiley-Blackwell; 2013:1330.
46. Acland GM, Aguirre GD, Ray J, et al. Gene therapy restores vision in a canine model of childhood blindness. *Nat Genet* 2001;28:92–95.
47. Aguirre GK, Komaromy AM, Cideciyan AV, et al. Canine and human visual cortex intact and responsive despite early retinal blindness from *RPE65* mutation. *PLoS Med*. 2007;4:e230.
48. Whiting RE, Narfstrom K, Yao G, et al. Pupillary light reflex deficits in a canine model of late infantile neuronal ceroid lipofuscinosis. *Exp Eye Res*. 2013;116:402–410.
49. Wong KY, Dunn FA, Berson DM. Photoreceptor adaptation in intrinsically photosensitive retinal ganglion cells. *Neuron*. 2005;48:1001–1010.
50. Flynn JT, Kazarian E, Barricks M. Paradoxical pupil in congenital achromatopsia. *Int Ophthalmol*. 1981;3:91–96.
51. Frank JW, Kushner BJ, France TD. Paradoxic pupillary phenomena. A review of patients with pupillary constriction to darkness. *Arch Ophthalmol*. 1988;106:1564–1566.
52. Price MJ, Thompson HS, Judisch GF, Corbett JJ. Pupillary constriction to darkness. *Br J Ophthalmol*. 1985;69:205–211.
53. Kankipati L, Girkin CA, Gamlin PD. Post-illumination pupil response in subjects without ocular disease. *Invest Ophthalmol Vis Sci*. 2010;51:2764–2769.
54. Kankipati L, Girkin CA, Gamlin PD. The post-illumination pupil response is reduced in glaucoma patients. *Invest Ophthalmol Vis Sci*. 2011;52:2287–2292.
55. Feigl B, Mattes D, Thomas R, Zele AJ. Intrinsically photosensitive (melanopsin) retinal ganglion cell function in glaucoma. *Invest Ophthalmol Vis Sci*. 2011;52:4362–4367.
56. Lei S, Goltz HC, Chandrakumar M, Wong AM. Full-field chromatic pupillometry for the assessment of the postillumination pupil response driven by melanopsin-containing retinal ganglion cells. *Invest Ophthalmol Vis Sci*. 2014;55:4496–4503.
57. van der Meijden WP, Te Lindert BH, Bijlenga D, et al. Post-illumination pupil response after blue light: Reliability of optimized melanopsin-based phototransduction assessment. *Exp Eye Res*. 2015;139:73–80.
58. McDougal DH, Gamlin PD. The influence of intrinsically-photosensitive retinal ganglion cells on the spectral sensitivity and response dynamics of the human pupillary light reflex. *Vision Res*. 2010;50:72–87.
59. Watson AB, Yellott JI. A unified formula for light-adapted pupil size. *J Vis* 2012;12:12.
60. Marg E, Morgan MW Jr. The pupillary near reflex; the relation of pupillary diameter to accommodation and the various components of convergence. *Am J Optom Arch Am Acad Optom*. 1949;26:183–198.
61. Bradley MM, Miccoli L, Escrig MA, Lang PJ. The pupil as a measure of emotional arousal and autonomic activation. *Psychophysiology*. 2008;45:602–607.
62. Kardon RH, Hong S, Kawasaki A. Entrance pupil size predicts retinal illumination in darkly pigmented eyes, but not lightly pigmented eyes. *Invest Ophthalmol Vis Sci*. 2013;54:5559–5567.
63. Chen Y, Kardon RH. Studying the effect of iris mechanics on the pupillary light reflex using brimonidine-induced anisocoria. *Invest Ophthalmol Vis Sci*. 2013;54:2951–2958.
64. Kim J, Heo J, Ji D, Kim MS. Quantitative assessment of pupillary light reflex in normal and anesthetized dogs: a preliminary study. *J Vet Med Sci*. 2015;77:475–478.
65. Gunderson EG, Lukasik VM, Ashton MM, Merideth RE, Madsen R. Effects of anesthetic induction with midazolam-propofol and midazolam-etomidate on selected ocular and cardiorespiratory variables in clinically normal dogs. *Am J Vet Res*. 2013;74:629–635.
66. Stephan DD, Vestre WA, Stiles J, Krohne S. Changes in intraocular pressure and pupil size following intramuscular administration of hydromorphone hydrochloride and acepromazine in clinically normal dogs. *Vet Ophthalmol*. 2003;6:73–76.
67. Switonski M. Dog as a model in studies on human hereditary diseases and their gene therapy. *Reprod Biol*. 2014;14:44–50.
68. Lorenz B, Gyurus P, Preising M, et al. Early-onset severe rod-cone dystrophy in young children with RPE65 mutations. *Invest Ophthalmol Vis Sci*. 2000;41:2735–2742.
69. Bainbridge JW, Smith AJ, Barker SS, et al. Effect of gene therapy on visual function in Leber's congenital amaurosis. *N Engl J Med*. 2008;358:2231–2239.
70. Maguire AM, Simonelli F, Pierce EA, et al. Safety and efficacy of gene transfer for Leber's congenital amaurosis. *N Engl J Med*. 2008;358:2240–2248.
71. Hauswirth WW, Aleman TS, Kaushal S, et al. Treatment of leber congenital amaurosis due to RPE65 mutations by ocular subretinal injection of adeno-associated virus gene vector: short-term results of a phase I trial. *Hum Gene Ther*. 2008;19:979–990.
72. Simonelli F, Maguire AM, Testa F, et al. Gene therapy for Leber's congenital amaurosis is safe and effective through 1.5 years after vector administration. *Mol Ther*. 2010;18:643–650.

Investigative Ophthalmology & Visual Science

73. Cideciyan AV, Hauswirth WW, Aleman TS, et al. Human RPE65 gene therapy for Leber congenital amaurosis: persistence of early visual improvements and safety at 1 year. *Hum Gene Ther*. 2009;20:999–1004.

74. Jacobson SG, Cideciyan AV, Ratnakaram R, et al. Gene therapy for Leber congenital amaurosis caused by *RPE65* mutations: safety and efficacy in 15 children and adults followed up to 3 years. *Arch Ophthalmol*. 2012;130:9–24.

Investigative Ophthalmology & Visual Science